AGU PUBLICATIONS

Geophysical Research Letters

RESEARCH LETTER

10.1002/2015GL064508

Observed platelet ice distributions in Antarctic sea ice: An index for ocean-ice shelf heat flux

P. J. Langhorne[1], K. G. Hughes[1], A. J. Gough[1], I. J. Smith[1], M. J. M. Williams[2], N. J. Robinson[2], C. L. Stevens[2,3], W. Rack[4], D. Price[4], G. H. Leonard[5], A. R. Mahoney[6], C. Haas[7], and T. G. Haskell[8]

[1]Department of Physics, University of Otago, Dunedin, New Zealand, [2]National Institute of Water and Atmospheric Research, Wellington, New Zealand, [3]Department of Physics, University of Auckland, Auckland, New Zealand, [4]Gateway Antarctica, University of Canterbury, Christchurch, New Zealand, [5]School of Surveying, University of Otago, Dunedin, New Zealand, [6]Geophysical Institute, University of Alaska Fairbanks, Fairbanks, Alaska, USA, [7]Earth & Space Science & Engineering Department, York University, Toronto, Ontario, Canada, [8]Callaghan Innovation, Wellington, New Zealand

Key Points:
- In SW Ross Sea no change in Ice Shelf Water volume under sea ice is detectable over past 100 years
- Using platelet ice records, an Antarctic-wide map of supercooled Ice Shelf Water is constructed
- Ice Shelf Water heat flux persists for months with a magnitude similar to that in polynya formation

Supporting Information:
- Data Set S2
- Data Set S1
- Data Sets 3 and 4, and Captions of Data Sets 1 and 2

Correspondence to:
P. J. Langhorne,
pat.langhorne@otago.ac.nz

Citation:
Langhorne, P. J., et al. (2015), Observed platelet ice distributions in Antarctic sea ice: An index for ocean-ice shelf heat flux, *Geophys. Res. Lett.*, *42*, 5442–5451, doi:10.1002/2015GL064508.

Received 11 MAY 2015
Accepted 19 JUN 2015
Accepted article online 23 JUN 2015
Published online 14 JUL 2015

Abstract Antarctic sea ice that has been affected by supercooled Ice Shelf Water (ISW) has a unique crystallographic structure and is called platelet ice. In this paper we synthesize platelet ice observations to construct a continent-wide map of the winter presence of ISW at the ocean surface. The observations demonstrate that, in some regions of coastal Antarctica, supercooled ISW drives a negative oceanic heat flux of -30 W m^{-2} that persists for several months during winter, significantly affecting sea ice thickness. In other regions, particularly where the thinning of ice shelves is believed to be greatest, platelet ice is not observed. Our new data set includes the longest ice-ocean record for Antarctica, which dates back to 1902 near the McMurdo Ice Shelf. These historical data indicate that, over the past 100 years, any change in the volume of very cold surface outflow from this ice shelf is less than the uncertainties in the measurements.

1. Introduction

Ice shelf basal melting is the largest ablation process in Antarctica [*Rignot et al.*, 2013; *Depoorter et al.*, 2013]. This process freshens and cools the fluid in the ice shelf-ocean boundary layer, producing Ice Shelf Water (ISW) that has a potential temperature below the surface freezing point [*Foldvik and Kvinge*, 1974; *Jacobs et al.*, 1985]. If the ISW moves to shallower depths, the rise in its pressure-dependent freezing point may force it to become supercooled in situ, causing ice crystals to persist and leading to the possibility of buoyancy-driven instability [*Jordan et al.*, 2015]. These frazil ice crystals collect under the ice shelf [e.g., *Craven et al.*, 2014], and if ocean currents are favorable, they are also carried out from the ice shelf cavity and deposited beneath neighboring sea ice [e.g., *Tison et al.*, 1998; *Gow et al.*, 1998; *Günther and Dieckmann*, 1999; *Robinson et al.*, 2014]. If they continue to be bathed in supercooled water, the crystals grow [e.g., *Wright and Priestley*, 1922; *Treshnikov*, 1963]. This is most apparent close to the sea ice-water interface where the potential for pressure-induced in situ supercooling is greatest [*Leonard et al.*, 2006, 2011]. The crystals, including ice that has been advected into place and ice that has grown in situ [*Dempsey et al.*, 2010; *Smith et al.*, 2012; *Gough et al.*, 2012a], may form a sub-ice platelet layer: a porous and friable layer in an evolving state of consolidation [*Moreçki*, 1965; *Crocker and Wadhams*, 1989] (Figure 1). Particle scavenging during the rise of frazil crystals, combined with the large surface area of the crystals and the ease of nutrient exchange in the porous sub-ice platelet layer, means that this habitat harbors some of the highest concentrations of sea ice algae on Earth [*Arrigo et al.*, 2010]. An algal "superbloom" can therefore be linked to its presence [*Smetacek et al.*, 1992; *Bombosch*, 1998].

However, supercooling alone is not sufficient for the formation of a sub-ice platelet layer. The modeling of *Dempsey et al.* [2010] suggested that a critical flux of ice crystals from the ocean must be exceeded and that this flux depends on the rate at which the solid, upper part of the sea ice is growing; i.e., a sub-ice platelet layer only forms when the conductive heat flux to the atmosphere is sufficiently low. This picture has been confirmed by observation [*Mahoney et al.*, 2011; *Gough et al.*, 2012a].

Incorporated platelet ice is formed when the water between the crystals of the sub-ice platelet layer freezes [*Jeffries et al.*, 1993; *Gow et al.*, 1998; *Smith et al.*, 2001]. Thus, we refer to ice crystals in the water column as frazil and define incorporated platelet ice and the sub-ice platelet layer as in Figure 1. We use "platelet ice" as the generic term for the latter two cases. While platelet ice is forming, the water a few centimeters below the tips of

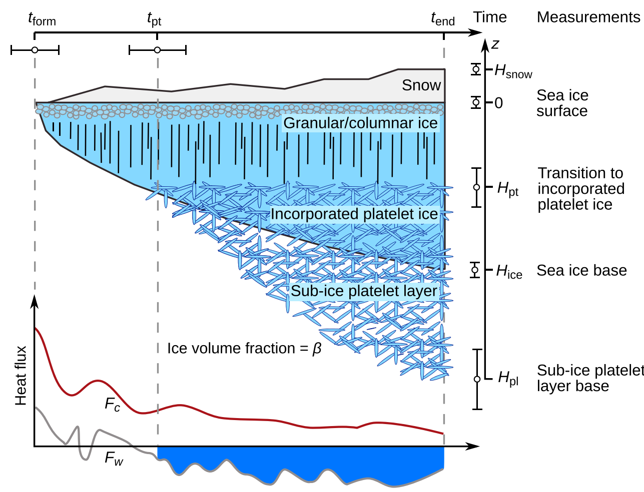

Figure 1. Schematic diagram of the development of incorporated platelet ice and a sub-ice platelet layer. Time progresses from left to right, with the time of initial sea ice formation given by t_{form}. At the end of winter (t_{end}) with $z = 0$ at the sea ice surface, the vertical location (positive upward) of the snow (H_{snow}), transition from granular or columnar ice to incorporated platelet ice (H_{pt}), sea ice base (H_{ice}), and the base of the sub-ice platelet layer (H_{pl}) are shown, each with an uncertainty. The change from columnar ice to incorporated platelet ice takes place at time t_{pt}. The conductive heat flux, F_c, and oceanic heat flux, F_w, are indicated. The heat to the ocean, integrated over winter (shaded in blue), can be calculated from the total thickness of platelet ice and its solid fraction, β (figure adapted from *Gough* [2012]).

the crystals is supercooled. Conversely, the persistent absence of supercooling implies an absence of platelet ice [*Smith et al.*, 2001]. Sea ice crystallography is therefore very sensitive to the presence of supercooled ISW and retains the history of some of the properties of the near-surface ocean during its winter freezing. Other physical properties, such as sea ice salinity, are insensitive [*Gough et al.*, 2012b].

Platelet ice causes sea ice to be thicker than it would otherwise be [*Smith et al.*, 2012; *Hoppmann et al.*, 2015a]. In late winter, in first year sea ice close to an ice shelf, at least 0.25 m of the 2 m thick cover forms due to heat loss to the ocean [*Purdie et al.*, 2006; *Gough et al.*, 2012a]. Similarly, multiyear fast ice, attached to the Mertz Glacier tongue, was estimated to be between 10 and 55 m thick, and frazil accumulation must have contributed to its thickness [*Massom et al.*, 2010].

Sea ice thickness is also influenced by the stabilization of the upper water column by meltwater in front of an ice shelf. Using an ocean model with ice shelf cavity thermodynamics, *Hellmer* [2004] predicted that sea ice is up to 0.2 m thicker for this reason. Since ice shelves occupy 44% of the coastline [*Drewry et al.*, 1982], this affects large areas of the Southern Ocean. While the influence on sea ice thickness is well established, the contribution of ice shelf melting as a factor in the unexplained discrepancy between global climate models and satellite-derived sea ice extent around Antarctica is more controversial [*Bintanja et al.*, 2013; *Swart and Fyfe*, 2013; *Holland et al.*, 2014]. We conclude that a heat flux to the ocean, the spatial distribution of surface supercooling, and the distribution of platelet ice are all manifestations of the same physical process.

One aim of this paper is to explore the *observational* evidence for the presence of supercooled ISW at the surface of the Southern Ocean by choosing near-surface oceanic heat flux as a suitable index from which to construct a continent-wide map. The implication is that sea ice at these locations may grow thicker due to an additional heat loss to the ocean. A second aim is to examine decadal-scale temporal changes by recognizing that the presence of platelet ice in Antarctic coastal sea ice is a measure of the heat deficit in an ice shelf cavity. In one location, historical data allow us to compare present-day conditions with those over a century ago.

2. Methods

2.1. Calculation of Oceanic Heat Flux as an Index for Supercooled ISW

We choose oceanic heat flux calculated from sea ice measurements as the most appropriate quantifiable index, arguing that it is one immediate measure of change to the rate of ice shelf basal melting and refreezing. The heat flux to the ocean is calculated under the assumption that all the ice of the sub-ice platelet layer and a fraction of the incorporated platelet ice have been formed due to heat loss to the water column (see Figure 1). At time t_{end}, toward the end of winter, the vertical locations of the transition to incorporated platelet ice (H_{pt}), the sea ice base (H_{ice}), and sub-ice platelet layer base (H_{pl}) may be determined. As winter progresses, the oceanic heat flux, F_w, changes from positive to negative (i.e., downward into the ocean), and at approximately this time, t_{pt}, a sub-ice platelet layer first forms below the sea ice. The conductive heat flux through the sea ice, F_c, decreases with time principally because the sea ice, with its snow cover, becomes thicker.

The average negative heat flux over the last few months of winter may be estimated from measurements of the thickness of the platelet ice, using

$$\langle F_w \rangle = \frac{\left(H_{pl} - H_{pt}\right) \beta \rho_{ice} L_{ice}}{t_{end} - t_{pt}} \tag{1}$$

where ρ_{ice} and L_{ice} are the density and latent heat of ice within the sub-ice platelet layer, for which we use values for pure ice (as described in *Gough* [2012]). $\left|H_{pl} - H_{pt}\right|$ is the total thickness of the platelet ice and includes any fraction that has been incorporated into the sea ice structure by advancing congelation ice. β is the ice volume fraction within a sub-ice platelet layer, or the fraction of the incorporated platelet ice that was formed due to heat loss to the water column. β is assumed to be a constant [*Smedsrud and Skogseth*, 2006].

Crystallographic examination of sea ice structure yields the thickness at which incorporated platelet ice first occurs in a sea ice core (H_{pt}). If we can trace back the thickness history of the sea ice, this can be used to approximate t_{pt}. Once a sub-ice platelet layer is established, and assuming that supercooled water continues to be present beneath the sea ice [*Leonard et al.*, 2011], the sub-ice platelet layer (at depth H_{pl}) advances faster than the ice (at depth H_{ice}). From studies of platelet ice formation in McMurdo Sound and as argued in *Gough* [2012], we assume that the sub-ice platelet layer begins to grow at the start of July when the sea ice thickness is H_{pt} = 1.50 m. Thus, a single pair (H_{pt}, t_{pt}) is used instead of many possible combinations. H_{pt} and t_{pt} are combined in $\frac{(H_{pl}-H_{pt})}{t_{end}-t_{pt}}$ in equation (1), and the error in this effective growth rate is considered to be approximately 35% [*Gough*, 2012]. Occasionally multiyear sea ice has been sampled, and *Gough* [2012] discusses the treatment of such data.

There is a large uncertainty in the ice volume fraction, where a range of values have been determined by different methods: heat flux from sea ice temperatures $\beta = 0.25 \pm 0.06$ [*Gough et al.*, 2012a], freeboard and thickness measurements $\beta = 0.16 \pm 0.07$ [*Price et al.*, 2014], platelet layer conductivity from multifrequency electromagnetic induction sounding $\beta = 0.29$–0.43 [*Hunkeler et al.*, 2015], buoyancy and volume measurements of ice crystals on ropes $\beta = 0.25$–0.30 [*Mahoney et al.*, 2011], frazil/grease ice samples from a polynya $\beta \sim 0.25$ [*Smedsrud and Skogseth*, 2006], comparison of modeled and observed sea ice growth rates $\beta = 0.25 \pm 0.10$ [*Hoppmann et al.*, 2015b], and modeling $\beta \sim 0.22$ [*Wongpan et al.*, 2015]. Noting this range of values, we choose $\beta = 0.25 \pm 0.09$ (uncertainty of 36%), which combines with the uncertainty in $\frac{(H_{pl}-H_{pt})}{t_{end}-t_{pt}}$ to give an uncertainty in $\langle F_w \rangle$ of approximately 50%.

2.2. Other Data Sources

The data set that has been compiled for this project (see supporting information) identifies the influence on sea ice of supercooled ISW at the ocean surface through (i) observations of frazil ice in the near-surface ocean and on objects submerged in the water, (ii) the acoustic or visual detection of frazil ice in the water column, (iii) the presence of an algal superbloom that can be linked to the presence of platelet ice, (iv) measurements of the thickness of the sub-ice platelet layer, and (v) crystallographic records from sea ice cores. All Antarctic sea ice cores for which there is a description of the crystallographic structure of the sea ice are included. We do not include cores if there is no crystallographic information.

3. Results

Positive observations of frazil and platelet ice at the ocean surface in Figure 2a (see supporting information for sources) coincide with locations where there is colder water at a depth of 200 m (i.e., less than 0.5°C above the surface freezing point) from the World Ocean Circulation Experiment data [*Gouretski and Koltermann*, 2004]. Negative observations are those where sea ice structure does not contain any signature of platelet ice. Data

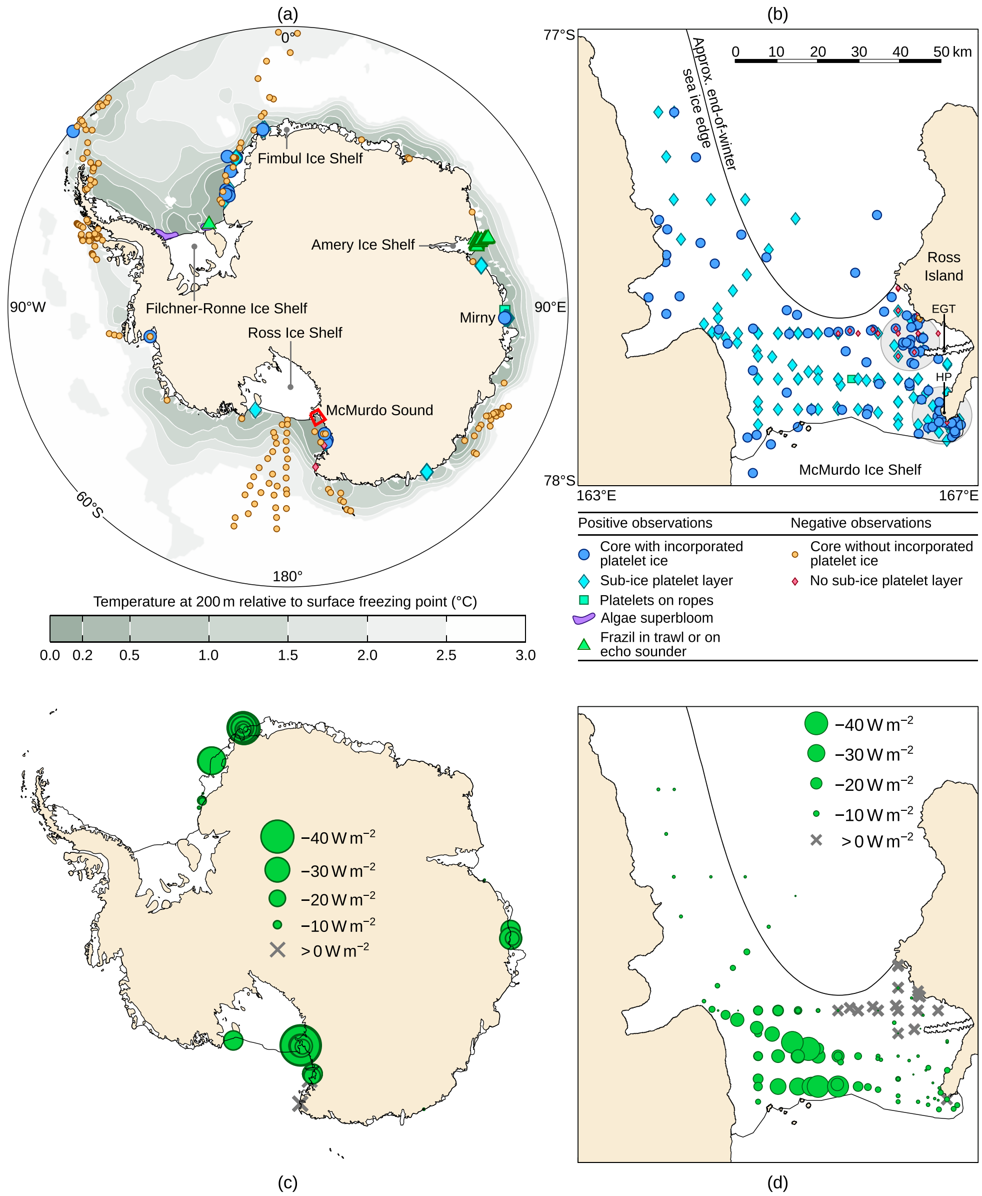

Figure 2. (a) Positive (in blue, green, and purple) observations of frazil and platelet ice in land-fast and drifting sea ice around Antarctica. Negative (in red and orange) observations imply sea ice structure reported without platelet ice. Data are plotted on a background of ocean temperature at 200 m relative to surface freezing point [*Gouretski and Koltermann*, 2004]. (b) Expanded and inverted view of McMurdo Sound (shown by red outline in Figure 2a). The shaded regions Erebus Glacier Tongue (EGT) and Hut Point (HP) are referred to in Figure 4. (c) Oceanic heat flux around Antarctica and (d) McMurdo Sound, derived from platelet ice measurements using equation (1). Note that $-10\ \mathrm{W\,m^{-2}}$ is equivalent to $\sim 3\ \mathrm{mm\,d^{-1}}$ growth of solid ice.

have been collected from 1902 until 2013, with the densest concentration of data in the southwestern Ross Sea (shown expanded and inverted in Figure 2b). In addition to McMurdo Sound, extreme examples of surface supercooling are seen near Mirny [*Moreçki*, 1965] where ice has been observed on ropes from the surface to 52 m.

In some regions of Antarctica there are few measurements. Where there are sufficient data to use equation (1), we show late-winter oceanic heat flux around Antarctica (see Figure 2c). To provide context, we note that $-10\ \mathrm{W\,m^{-2}}$ is equivalent to $\sim 3\ \mathrm{mm\,d^{-1}}$ growth of solid ice. As expected, all negative heat fluxes are close to the outflow region of a major ice shelf.

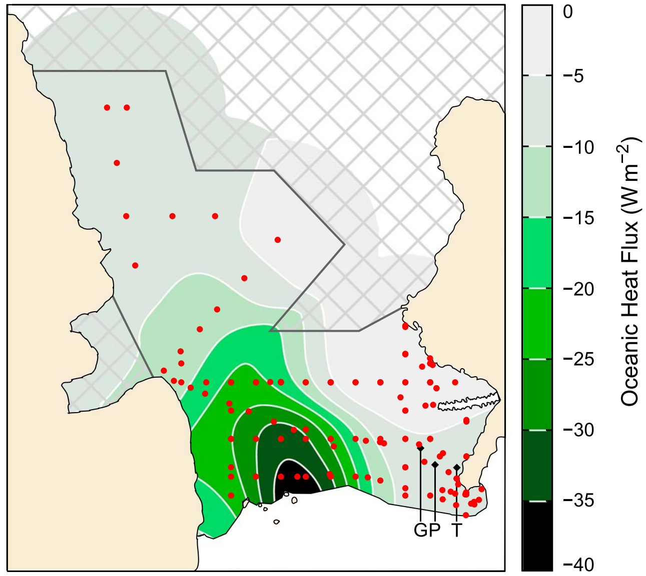

Figure 3. Oceanic heat flux in McMurdo Sound calculated at sites shown by red dots from equation (1) with $\beta = 0.25$ and interpolated using a Gaussian weighting function. Contoured data are principally from 1986 [*Crocker*, 1988], 2009 [*Gough*, 2012], 2011 [*Price et al.*, 2014; *Hughes et al.*, 2014], and 2013. In addition, various smaller data sets of sub-ice platelet layer thickness are included from the literature (see supporting information). In 2011 and 2013, five measurements were averaged for each value of H_{ice} and H_{pl} [*Price et al.*, 2014; *Hughes et al.*, 2014]. Late-winter oceanic heat fluxes, deduced from sea ice temperature measurements, were $\langle F_w \rangle \approx -10$ W m^{-2} in 1997 and 1999 at site T [*Trodahl et al.*, 2000; *Smith et al.*, 2012] and 2009 at site G [*Gough et al.*, 2012a] and $\langle F_w \rangle \approx -5$ W m^{-2} in 2003 at site P [*Purdie et al.*, 2006]. Cross hatching indicates regions where the uncertainty in oceanic heat flux is greater than ± 50%.

The paucity of observations in Figure 2c may be because there are few places where there is significant negative oceanic heat flux at the surface. In some regions near massive ice shelves, such as around parts of the Filchner-Ronne or Amery Ice Shelves, the ISW emerges at depth [e.g., *Dieckmann et al.*, 1986; *Nicholls et al.*, 2009; *Shi et al.*, 2011; *Zheng et al.*, 2011]. To be detectable in this study, the ISW must reach the ocean surface before the very cold water is warmed by exchange with the surrounding ocean. In other cases water that is seasonally warmer than the freezing point interacts with the ice shelf front at shallow depths [*Jacobs et al.*, 1992], driven downward by processes such as wind forcing. Observations indicate that this is happening below the Fimbul Ice Shelf [*Hattermann et al.*, 2012] and provides a possible explanation for the lack of platelet ice in this region. Platelet ice formation may also be masked by the frequent existence of a polynya at an ice shelf front. Alternatively, there may simply be insufficient data coverage around the continent. McMurdo Sound (Figures 2b and 2d) is well placed as an outflow region for the Ross Ice Shelf cavity [*Robinson et al.*, 2014; *Hughes et al.*, 2014], and we examine this location in more detail.

3.1. McMurdo Sound: Spatial Distribution of Oceanic Heat Flux (1986–2013)

Observations of platelet ice are particularly common in McMurdo Sound in the southwestern Ross Sea [e.g., *Paige*, 1966; *Crocker*, 1988; *Jeffries et al.*, 1993; *Gow et al.*, 1998; *Gough et al.*, 2012a; *Hughes et al.*, 2014]. The mean, late-winter, oceanic heat flux deduced from equation (1) is shown in Figure 3. Contours of heat flux are in agreement with late-winter oceanic heat fluxes, deduced from sea ice temperature measurements [*Trodahl et al.*, 2000; *Purdie et al.*, 2006; *Smith et al.*, 2012; *Gough et al.*, 2012a].

3.2. McMurdo Sound: Temporal Evolution of Oceanic Heat Flux (1902–2013)

McMurdo Sound observations of (i) the presence (or absence) of incorporated platelet ice in sea ice cores, (ii) the thickness of a sub-ice platelet layer, and (iii) ice attached to ropes and lines submerged in the water column are all used as proxies for the volume of platelet ice from 1902 to 2013 (Figure 4). Only observations within 7 km of Hut Point (HP) or the Erebus Glacier Tongue (EGT) (measurements within shaded circles in Figure 2b) are used in the times series so that the data are not influenced by the effects of the spatial distribution of $\langle F_w \rangle$ (Figure 3). These two sites experience conditions that are consistent with our schematic diagram (Figure 1), i.e., first year sea ice with summer ocean surface temperatures above the freezing point.

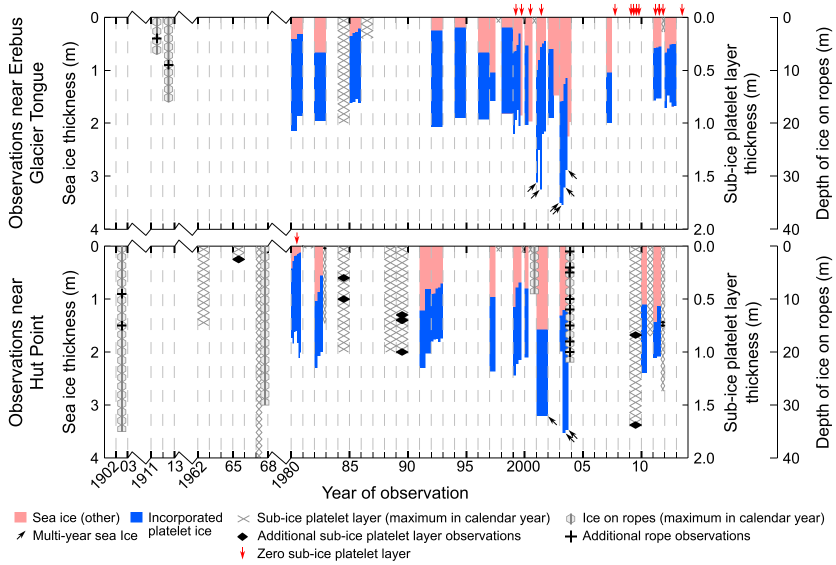

Figure 4. Timeline of sea ice observations in McMurdo Sound, 1902–2013, at sites within the shaded regions near EGT (Erebus Glacier Tongue) and HP (Hut Point) as shown in Figure 2b. Data compiled from sea ice structure, with incorporated platelet ice in cores in blue at bottom and other ice types in red above; sub-ice platelet layer thickness (shown as grey crosses); and maximum annual ice accumulated on ropes (shown as grey hexagons). For some years there are multiple observations of ice on ropes/sub-ice platelet layer. Maximum depths have been indicated with the shallower depths being marked as pluses/diamonds. Instances where there is an absence of a sub-ice platelet layer are shown as red arrows. All data are first year sea ice except where identified as multiyear ice.

These observations are supplemented with near-surface winter oceanographic measurements (within 50 m of the ocean surface), beginning with the 1911 measurements of Nelson [*Deacon*, 1975]. Figure 5a shows that, within measurement error, winter ocean surface temperature appears unchanged since the early 1900s (see data sources in the supporting information), while the salinity within the upper 50 m of the water column (Figure 5b) has probably decreased after the 1960s. The change that this makes to the freezing temperature is within the error of the historical measurements. Consequently, ocean surface temperatures have been held 10–20 mK below the surface freezing point (Figure 5c) from June to November in 1960 and in 2009, implying little temperature change over five decades.

4. Discussion

4.1. Oceanic Heat Flux Index Reliability

In this work we have selected the mean late-winter oceanic heat flux as a quantifiable index, arguing that this is one immediate measure of change to ice shelf basal melting and refreezing. Instead, we might have chosen to calculate the total thermal energy involved in the freezing of platelet ice (in MJ m^{-2} $annum^{-1}$). In contrast to the thermal energy, the oceanic heat flux used here is insensitive to the precise time of year at which the observations are made, because platelet ice thickness and observation date are linked. As a result, there would be greater uncertainty in the calculation of thermal energy than in heat flux. We now explore the reliability of the heat flux index we have constructed.

In McMurdo Sound, the pattern of oceanic heat flux (Figure 3) mimics previous measures of late-winter surface supercooling [*Lewis and Perkin*, 1985], qualitative observations of the relative distribution of crystals observed on ropes and under sea ice [*Barry*, 1988], and the relative abundance of platelet ice in cores [*Dempsey et al.*, 2010]. This pattern is known to be driven by the circulation in the Sound [*Barry*, 1988; *Dempsey et al.*, 2010; *Robinson et al.*, 2010, 2014]. More importantly, there is also good agreement between the magnitude of our constructed oceanic heat flux (Figure 3) and measurements derived from sea ice temperatures in eastern McMurdo Sound [*Trodahl et al.*, 2000; *Purdie et al.*, 2006; *Gough et al.*, 2012a; *Smith et al.*, 2012]. The persistence of ISW influence beyond the ice shelf front also concurs with estimates in excess of 200 km, derived from salt diffusivity and current measurements [*Stevens et al.*, 2009] and from modeling [*Hughes et al.*, 2014]. Thus, the

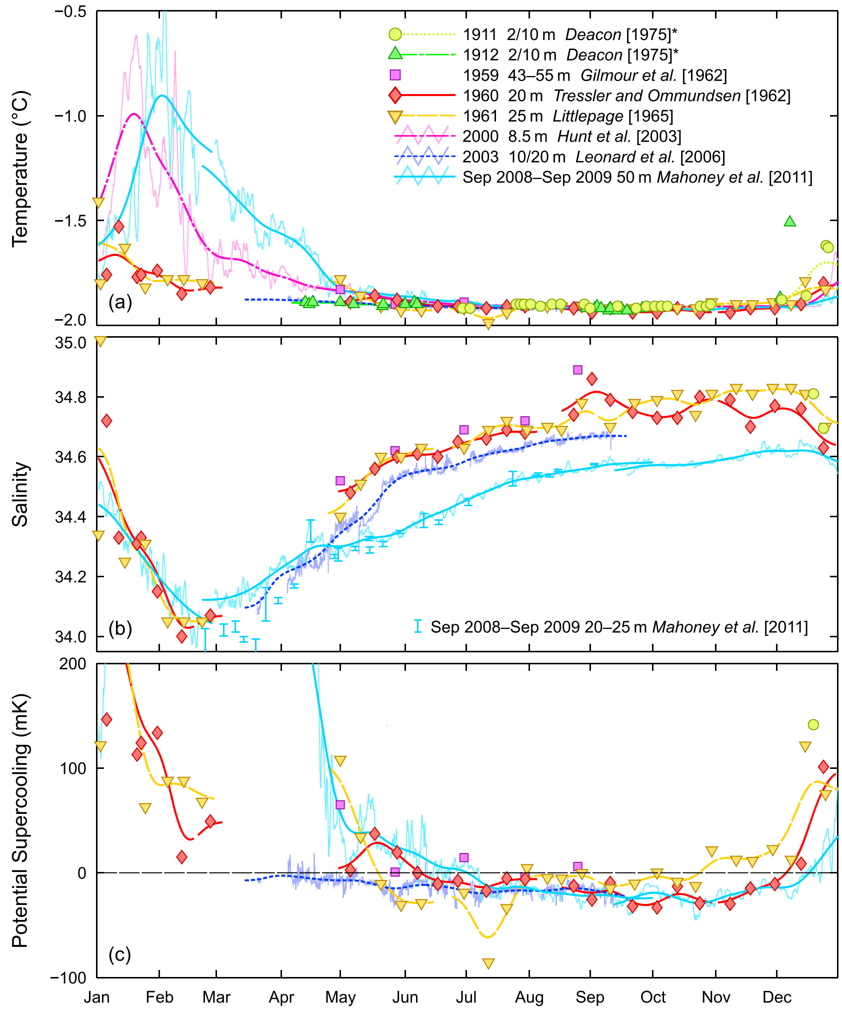

Figure 5. Seasonal variation in surface ocean (a) temperature, (b) salinity, and (c) potential supercooling in McMurdo Sound from 1911 to present. Data were smoothed with a Gaussian weighting function with σ = 7 days. Asterisks indicate *Deacon* [1975] reported data collected by E. W. Nelson.

agreement between the heat flux index and the available measurements (Figure 3) gives us confidence to extrapolate our ideas to historical and continent-wide estimates.

Modeling has shown that an increase in flux of supercooled ISW causes a thicker sub-ice platelet layer [*Hughes et al.*, 2014], while the thickness of incorporated platelet ice in sea ice cores records the length of time that surface ISW is present each year [*Leonard et al.*, 2006; *Mahoney et al.*, 2011]. Consequently, we conclude that the thickness of the incorporated platelet ice and the sub-ice platelet layer are correlated with the volume of supercooled ISW emerging from the cavity in 1 year. While the century-long sea ice record is not of sufficient quality to derive a quantitative index, it indicates that there is little evidence of change in the thickness of platelet ice in eastern McMurdo Sound in the period 1902–2013 (Figure 4). This is confirmed by the supercooling measurements in winter (April to November) shown in Figure 5c. There also appears to have been little change in winter ocean surface temperature in McMurdo Sound between 1911 and 2009, while the salinity within the upper 50 m of the water column has probably decreased. The 2003 record is influenced by the temporary presence of giant icebergs [*Robinson and Williams*, 2012], but comparing 1960 winter salinity measurements with those of 2009 yields a decrease of ~0.04 decade^{-1}. This is in agreement with an observed decrease in summer salinity of 0.03 decade^{-1} at depths below 200 m in the southwestern Ross Sea (1958–2008) [*Jacobs and Giulivi*, 2010]. In spite of the freshening, ocean surface temperatures are held 10–20 mK below the freezing point during winter (Figure 5c), due to the efficiency of frazil formation, the presence of crystallization nuclei and the regulating influence of basal melting in the ice shelf cavity.

4.2. Relationship of Oceanic Heat Flux Index to Present-Day Antarctica

The derived heat fluxes are of similar magnitude, but opposite in sense, to those involved in polynya formation. For example, the oceanic heat flux in McMurdo Sound is similar to the areal mean heat flux of 25 W m^{-2} which maintained the Maud Rise sensible heat polynya in the eastern Weddell Sea [*Muench et al.*, 2001]. Clearly a flow of heat to the ocean is important near ice shelves and leads to thicker sea ice than would otherwise be found around coastal Antarctica. In turn, more energy must be required to melt sea ice in the regions identified on our map (Figure 2c). Our results provide observational evidence of the important role of ISW, which needs to be considered in regional models of the ocean or sea ice.

There are also implications for the stability of ice shelves. Deposits, similar to platelet ice, make a significant contribution to the thickness of the major ice shelves [e.g., *Bombosch*, 1998]. The presence of platelet ice in the sea ice can be a signature of these deposits extending beyond the ice shelf front, and its absence correlates well with those regions where the thinning of ice shelves is believed to be greatest [e.g., *Paolo et al.*, 2015].

4.3. Future Measurements

Our knowledge of the pervasiveness of the influence of ISW is limited by the paucity of measurements. A remote sensing approach might resolve this limitation. Under first year sea ice, it has been shown that it is possible to detect the sub-ice platelet layer using electromagnetic induction techniques [*Rack et al.*, 2013; *Hunkeler et al.*, 2015], and this offers promise for more extensive surveys using aircraft. Currently the indirect detection of the platelet layer is at the limits of resolution for satellite altimetry [*Price et al.*, 2014], although it is indicated that a thick sub-ice platelet layer beneath coastal fast ice is identifiable in McMurdo Sound, where freeboard anomalies were found to coincide with the sub-ice platelet layer [*Price et al.*, 2013]. However, if airborne and satellite remote sensing estimates of the extent of influence of ISW are to be made, they need to be supported by in situ observation, and supplemented by modeling at a range of scales.

5. Conclusion

The volume of supercooled ISW at the ocean surface is not only a measure of processes taking place beneath the ice shelf, but it also influences the state of the sea ice, its thickness, and longevity. The inclusion of platelet ice into first year sea ice is an annual process and hence will be an immediate response to changes in the sub-ice shelf circulation pattern and its export of supercooled water. Further, platelet ice enhances primary production as it hosts the highest concentrations of sea ice algae to be found on Earth [*Arrigo et al.*, 2010]. Any change in the highly productive platelet ice habitat in a warming ocean will have consequential effects across the rest of the Southern Ocean ecosystem. Yet the pervasiveness of platelet ice, subsurface supercooling, and negative oceanic heat flux around Antarctica have previously been poorly known.

In this paper we have combined data from a range of sources, including some of the first Antarctic geophysical measurements from more than a century ago, to formulate an oceanic heat flux index as a measure of the presence of supercooled ISW at the ocean surface. The derived negative ocean heat fluxes associated with platelet ice growth are comparable in magnitude to heat fluxes associated with well-known recurring polynyas. We have constructed a continent-wide map that reflects the production and transport of ISW, which may be used to evaluate ice shelf-ocean modeling, and models that estimate primary productivity.

The most extensive data set, which includes our new results, extends north of the combined Ross and McMurdo Ice Shelf front in the southern Ross Sea. Here the surface water is held just below its freezing point as it enters McMurdo Sound from beneath the McMurdo Ice Shelf. Since the early twentieth century there has been no detectable change in the volume or temperature of this supercooled ISW under sea ice, a result in keeping with changes in the satellite altimeter-determined thickness of the western Ross Ice Shelf (1994–2012) [*Paolo et al.*, 2015]. For the 100 years of the record, this implies that the catastrophic ocean warming and ice shelf mass loss that is being seen in the Amundsen Sea region [e.g., *Jacobs et al.*, 2011; *Sutterley et al.*, 2014] has not yet been felt by the southwestern Ross Sea, emphasizing the urgent need for careful, Antarctic-wide monitoring.

Acknowledgments
Previously unpublished data were collected in McMurdo Sound with the support of Antarctica New Zealand and the winter-over crews of 2003 and 2009. A contribution to the collection of these Antarctic field data was made by Brett Grant, Stefan Jendersie, Justin Beckers, Kelvin Barnsdale, Jono Leitch, and Brian Staite. Contributions to the formulation of ideas in this work were made by Pat Wongpan, Stefan Jendersie, David Dempsey, Craig Purdie, Cecilia Bitz, Lars Smedsrud, Stephen Ackley, and Mario Hoppmann. Project support was supplied by the New Zealand Ministry of Science and Innovation, Foundation for Research Science and Technology, National Institute of Water and Atmospheric Research, and the Universities of Otago and Canterbury. The data compiled for this study may be accessed in the supporting information.

The Editor thanks Stephen Ackley and an anonymous reviewer for their assistance in evaluating this paper.

References

Arrigo, K. R., T. Mock, and M. P. Lizotte (2010), Primary producers and sea ice, in *Sea Ice*, edited by D. N. Thomas and G. S. Dieckmann, pp. 283–326, Wiley, Oxford, U. K.

Barry, J. P. (1988), Hydrographic patterns in McMurdo Sound, Antarctica and their relationship to local benthic communities, *Polar Biol.*, *8*(5), 377–391, doi:10.1007/BF00442029.

Bintanja, R., G. van Oldenborgh, S. Drijfhout, B. Wouters, and C. Katsman (2013), Important role for ocean warming and increased ice-shelf melt in Antarctic sea-ice expansion, *Nat. Geosci.*, *6*(5), 376–379, doi:10.1038/ngeo1767.

Bombosch, A. (1998), Interactions between floating ice platelets and ocean water in the southern Weddell Sea, in *Ocean, Ice, and Atmosphere: Interactions at the Antarctic Continental Margin, Antarct. Res. Ser.*, vol. 75, edited by S. S. Jacobs and R. F. Weiss, pp. 257–266, AGU, Washington, D. C., doi:10.1029/AR075p0257.

Craven, M., R. C. Warner, B. K. Galton-Fenzi, L. Herraiz-Borreguer, S. W. Vogel, and I. Allison (2014), Platelet ice attachment to instrument strings beneath the Amery Ice Shelf, East Antarctica, *J. Glaciol.*, *60*(220), 383–393, doi:10.3189/2014JoG13J082.

Crocker, G. B. (1988), Physical processes in Antarctic landfast sea ice, PhD thesis, Univ. of Cambridge, U. K.

Crocker, G. B., and P. Wadhams (1989), Modeling Antarctic fast-ice growth, *J. Glaciol.*, *35*(119), 3–8, doi:10.3189/002214389793701590.

Deacon, G. E. R. (1975), The oceanographical observations of Scott's last expedition, *Polar Rec.*, *17*(109), 391–419.

Dempsey, D. E., P. J. Langhorne, N. J. Robinson, M. J. M. Williams, T. G. Haskell, and R. D. Frew (2010), Observation and modeling of platelet ice fabric in McMurdo Sound, Antarctica, *J. Geophys. Res.*, *115*, C01007, doi:10.1029/2008JC005264.

Depoorter, M. A., J. L. Bamber, J. A. Griggs, J. T. M. Lenaerts, S. R. M. Ligtenberg, M. R. van den Broeke, and G. Moholdt (2013), Calving fluxes and basal melt rates of Antarctic ice shelves, *Nature*, *502*, 89–92, doi:10.1038/nature12567.

Dieckmann, G. S., G. Rohardt, H. H. Hellmer, and J. Kipfstuhl (1986), The occurrence of ice platelets at 250 m depth near the Filchner Ice Shelf and its significance for sea ice biology, *Deep Sea Res. Part A*, *33*(2), 141–148, doi:10.1016/0198-0149(86)90114-7.

Drewry, D. J., S. R. Jordan, and E. Jankowski (1982), Measured properties of the Antarctic ice sheet: Surface configuration, ice thickness, volume and bedrock characteristics, *Ann. Glaciol.*, *3*, 83–91.

Foldvik, A., and T. Kvinge (1974), Conditional instability of sea-water at freezing-point, *Deep Sea Res.*, *21*(3), 69–174, doi:10.1016/0011-7471(74)90056-4.

Gilmour, A. E., W. J. P. Macdonald, and F. G. van der Hoeven (1962), Winter measurements of sea currents in McMurdo Sound, *N. Z. J. Geol. Geophys.*, *5*(5), 778–789.

Gough, A. (2012), Sea ice near an ice shelf, PhD thesis, Univ. of Otago, Dunedin, New Zealand.

Gough, A. J., A. R. Mahoney, P. J. Langhorne, M. J. M. Williams, N. J. Robinson, and T. G. Haskell (2012a), Signatures of supercooling: McMurdo Sound platelet ice, *J. Glaciol.*, *58*(207), 38–50, doi:10.3189/2012JoG10J218.

Gough, A. J., A. R. Mahoney, P. J. Langhorne, M. J. M. Williams, and T. G. Haskell (2012b), Sea ice salinity and structure: A winter time series of salinity and its distribution, *J. Geophys. Res.*, *117*, C03008, doi:10.1029/2011JC007527.

Gouretski, V. V., and K. P. Koltermann (2004), WOCE Global Hydrographic Climatology, *Ber. Bundesamtes Seeschifffahrt Hydrogr., Tech. Rep.*, *35*, 1–52. Natl. Cent. for Atmos. Res., Comput. and Inf. Syst. Lab., Boulder, Colo.

Gow, A. J., S. F. Ackley, J. W. Govoni, and W. F. Weeks (1998), Physical and structural properties of land-fast sea ice in McMurdo Sound, Antarctica, in *Antarctic Sea Ice: Physical Processes, Interactions and Variability, Antarct. Res. Ser.*, vol. 74, edited by M. O. Jeffries, pp. 355–374, AGU, Washington, D. C., doi:10.1029/AR074p0355.

Günther, S., and G. S. Dieckmann (1999), Seasonal development of algal biomass in snow-covered fast ice and the underlying platelet layer in the Weddell Sea, Antarctica, *Antarct. Sci.*, *11*(3), 305–315, doi:10.1017/S0954102099000395.

Hattermann, T., O. A. Nøst, J. M. Lilly, and L. H. Smedsrud (2012), Two years of oceanic observations below the Fimbul Ice Shelf, Antarctica, *Geophys. Res. Lett.*, *39*, L12605, doi:10.1029/2012GL051012.

Hellmer, H. H. (2004), Impact of Antarctic ice shelf basal melting on sea ice and deep ocean properties, *Geophys. Res. Lett.*, *31*, L10307, doi:10.1029/2004GL019506.

Holland, P. R., N. Bruneau, C. Enright, M. Losch, N. T. Kurtz, and R. Kwok (2014), Modeled trends in Antarctic sea ice thickness, *J. Clim.*, *27*(10), 3784–3801, doi:10.1175/JCLI-D-13-00301.1.

Hoppmann, M., M. Nicolaus, P. A. Hunkeler, P. Heil, L. -K. Behrens, G. König-Langlo, and R. Gerdes (2015a), Seasonal evolution of an ice-shelf influenced fast-ice regime, derived from an autonomous thermistor chain, *J. Geophys. Res. Oceans*, *120*, 1703–1724, doi:10.1002/2014JC010327.

Hoppmann, M., et al. (2015b), Ice platelets below Weddell Sea land fast sea ice, *Ann. Glaciol.*, *56*(69), 175–190, doi:10.3189/2015AoG69A678.

Hughes, K. G., P. J. Langhorne, G. H. Leonard, and C. L. Stevens (2014), Extension of an Ice Shelf Water plume model beneath sea ice with application in McMurdo Sound, Antarctica, *J. Geophys. Res. Oceans*, *119*, 8662–8687, doi:10.1002/2013JC009411.

Hunkeler, P. A., S. Hendricks, M. Hoppmann, S. Paul, and R. Gerdes (2015), Towards an estimation of sub-sea-ice platelet-layer volume with multi-frequency electromagnetic induction sounding, *Ann. Glaciol.*, *56*(69), 137–146, doi:10.3189/2015AoG69A705.

Hunt, B. M., K. Hoefling, and C. C. Cheng (2003), Annual warming episodes in seawater temperatures in McMurdo Sound in relationship to endogenous ice in notothenioid fish, *Antarct. Sci.*, *15*(3), 333–338, doi:10.1017/S0954102003001342.

Jacobs, S. S., and C. F. Giulivi (2010), Large multidecadal salinity trends near the Pacific-Antarctic continental margin, *J. Clim.*, *23*(17), 4508–4524.

Jacobs, S. S., R. G. Fairbanks, and Y. Horibe (1985), Origin and evolution of water masses near the Antarctic continental margin: Evidence from $H_2^{18}O/H_2^{16}O$ ratios in seawater, in *Oceanology of the Antarctic Continental Shelf*, edited by S. S. Jacobs, AGU, Washington, D. C., doi:10.1029/AR043p0059.

Jacobs, S. S., H. H. Hellmer, C. S. M. Doake, A. Jenkins, and R. M. Frolich (1992), Melting of ice shelves and the mass balance of Antarctica, *J. Glaciol.*, *38*, 375–387.

Jacobs, S. S., A. Jenkins, C. F. Giulivi, and P. Dutrieux (2011), Stronger ocean circulation and increased melting under Pine Island Glacier ice shelf, *Nat. Geosci.*, *4*(8), 519–523, doi:10.1038/NGEO1188.

Jeffries, M. O., W. F. Weeks, R. Shaw, and K. Morris (1993), Structural characteristics of congelation and platelet ice and their role in the development of Antarctic land-fast sea ice, *J. Glaciol.*, *39*(132), 223–238.

Jordan, J. R., S. Kimura, P. R. Holland, A. Jenkins, and M. D. Piggott (2015), On the conditional frazil ice instability in seawater, *J. Phys. Oceanogr.*, *45*, 1121–1138, doi:10.1175/JPO-D-14-0159.1.

Leonard, G. H., C. R. Purdie, P. J. Langhorne, T. G. Haskell, M. J. M. Williams, and R. D. Frew (2006), Observations of platelet ice growth and oceanographic conditions during the winter of 2003 in McMurdo Sound, Antarctica, *J. Geophys. Res.*, *111*, C04012, doi:10.1029/2005JCC002952.

Leonard, G. H., P. J. Langhorne, M. J. M. Williams, R. Vennell, C. R. Purdie, D. E. Dempsey, T. G. Haskell, and R. D. Frew (2011), Evolution of supercooling under coastal Antarctic sea ice during winter, *Antarct. Sci.*, *23*(4), 399–409, doi:10.1017/S0954102011000265.

Lewis, E. L., and R. G. Perkin (1985), The winter oceanography of McMurdo Sound, Antarctica, in *Oceanology of the Antarctic Continental Shelf, Antarct. Res. Ser.*, edited by S. S. Jacobs, pp. 145–165, AGU, Washington, D. C.

Littlepage, J. L. (1965), Oceanographic investigations in McMurdo Sound, Antarctica, in *Biology of the Antarctic Seas II, Antarct. Res. Ser.*, vol. 5, edited by G. A. Llano, pp. 1–37, AGU, Washington, D. C.

Mahoney, A. R., A. J. Gough, P. J. Langhorne, N. J. Robinson, C. L. Stevens, M. J. M. Williams, and T. G. Haskell (2011), The seasonal appearance of ice shelf water in coastal Antarctica and its effect on sea ice growth, *J. Geophys. Res.*, *116*, C11032, doi:10.1029/2011JC007060.

Massom, R. A., A. B. Giles, H. A. Fricker, R. C. Warner, B. Legrésy, G. Hyland, N. Young, and A. D. Fraser (2010), Examining the interaction between multi-year landfast sea ice and the Mertz Glacier Tongue, East Antarctica: Another factor in ice sheet stability?, *J. Geophys. Res.*, *115*, C12027, doi:10.1029/2009JC006083.

Moreçki, V. N. (1965), Underwater sea ice, *Probl. Arkt. Antarkt.*, *19*, 32–38. English translation by E. R. Hope, DRB Canada Report No. T497R April, 1968.

Muench, R., J. Morison, L. Padman, D. Martinson, P. Schlosser, B. Huber, and R. Hohmann (2001), Maud Rise revisited, *J. Geophys. Res.*, *106*(C2), 2423–2440, doi:10.1029/2000JC000531.

Nicholls, K. W., S. Østerhus, K. Makinson, T. Gammelsrød, and E. Fahrbach (2009), Ice-ocean processes over the continental shelf of the southern Weddell Sea, Antarctica: A review, *Rev. Geophys.*, *47*, RG3003, doi:10.1029/2007RG000250.

Paige, R. A., (1966), Crystallographic studies of sea ice in McMurdo Sound, Antarctica, *Tech. Rep. R494*, U.S. Naval Civil Engineering Lab., Port Hueneme, Calif.

Paolo, F. S., H. A. Fricker, and L. Padman (2015), Volume loss from Antarctic ice shelves is accelerating, *Science*, *348*(6232), 327–331, doi:10.1126/science.aaa0940.

Price, D., W. Rack, C. Haas, P. J. Langhorne, and O. Marsh (2013), Sea ice freeboard in McMurdo Sound, Antarctica, derived by surface-validated ICESat laser altimeter data, *J. Geophys. Res. Oceans*, *118*, 3634–3651, doi:10.1002/jgrc.20266.

Price, D., W. Rack, P. J. Langhorne, C. Haas, G. Leonard, and K. Barnsdale (2014), The sub-ice platelet layer and its influence on freeboard to thickness conversion of Antarctic sea ice, *The Cryosphere*, *8*(1), 1031–1039, doi:10.5194/tc-8-1031-2014.

Purdie, C., P. Langhorne, G. Leonard, and T. Haskell (2006), Growth of first year land-fast Antarctic sea ice determined from winter temperature measurements, *Ann. Glaciol.*, *44*, 170–176, doi:10.3189/172756406781811853.

Rack, W., C. Haas, and P. J. Langhorne (2013), Airborne thickness and freeboard measurements over the McMurdo Ice Shelf, Antarctica, and implications for ice density, *J. Geophys. Res. Oceans*, *118*, 5899–5907, doi:10.1002/2013JC009084.

Rignot, E., S. Jacobs, J. Mouginot, and B. Scheuchl (2013), Ice-shelf melting around Antarctica, *Science*, *341*(6143), 266–270, doi:10.1126/science.1235798.

Robinson, N. J., and M. J. M. Williams (2012), Iceberg-induced changes to polynya operation and regional oceanography in the southern Ross Sea, Antarctica, from in situ observations, *Antarct. Sci.*, *24*(5), 514–526, doi:10.1017/S0954102012000296.

Robinson, N. J., M. J. M. Williams, P. J. Barrett, and A. R. Pyne (2010), Observations of flow and ice-ocean interaction beneath the McMurdo Ice Shelf, Antarctica, *J. Geophys. Res.*, *115*, C03025, doi:10.1029/2008JC005255.

Robinson, N. J., M. J. M. Williams, C. L. Stevens, P. J. Langhorne, and T. G. Haskell (2014), Evolution of a supercooled Ice Shelf Water plume with an actively growing subice platelet matrix, *J. Geophys. Res. Oceans*, *119*, 3425–3446, doi:10.1002/2013JC009399.

Shi, J., Y. Cheng, Y. Jiao, and J. Hou (2011), Supercooled water in austral summer in Prydz Bay, Antarctica, *Chin. J. Oceanol. Limnol.*, *29*(2), 427–437, doi:10.1007/s00343-010-0011-5.

Smedsrud, L., and R. Skogseth (2006), Field measurements of Arctic grease ice properties and processes, *Cold Reg. Sci. Technol.*, *44*(3), 171–183, doi:10.1016/j.coldregions.2005.11.002.

Smetacek, V., R. Scharek, L. I. Gordon, H. Eicken, E. Fahrbach, G. Rohardt, and S. Moore (1992), Early spring phytoplankton blooms in ice platelet layers of the southern Weddell Sea, Antarctica, *Deep Sea Res.*, *39*(2), 153–168, doi:10.1016/0198-0149(92)90102-Y.

Smith, I. J., P. J. Langhorne, T. G. Haskell, H. J. Trodahl, R. Frew, and R. Vennell (2001), Platelet ice and the land-fast sea ice of McMurdo Sound, Antarctica, *Ann. Glaciol.*, *33*, 21–27, doi:10.3189/172756401781818365.

Smith, I. J., P. J. Langhorne, R. D. Frew, R. Vennell, and T. G. Haskell (2012), Sea ice growth rates near ice shelves, *Cold Reg. Sci. Technol.*, *83–84*, 57–70, doi:10.1016/j.coldregions.2012.06.005.

Stevens, C. L., N. J. Robinson, M. J. M. Williams, and T. G. Haskell (2009), Observations of turbulence beneath sea ice in southern McMurdo Sound, Antarctica, *Ocean Sci.*, *4*, 435–445.

Sutterley, T. C., I. Velicogna, E. Rignot, J. Mouginot, T. Flament, M. R. van den Broeke, J. M. van Wessem, and C. H. Reijmer (2014), Mass loss of the Amundsen Sea Embayment of West Antarctica from four independent techniques, *Geophys. Res. Lett.*, *41*, 8421–8428, doi:10.1002/2014GL061940.

Swart, N. C., and J. C. Fyfe (2013), The influence of recent Antarctic ice sheet retreat on simulated sea ice area trends, *Geophys. Res. Lett.*, *40*, 4328–4332, doi:10.1002/grl.50820.

Tison, J.-L., R. D. Lorrain, A. Bouzette, M. Dini, A. Bondesan, and M. Stiévenard (1998), Linking landfast sea ice variability to marine ice accretion at Hells Gate Ice Shelf, Ross Sea, in *Antarctic Sea Ice: Physical Processes, Interactions and Variability, Antarct. Res. Ser.*, vol. 74, edited by M. O. Jeffries, pp. 375–407, AGU, Washington, D. C.

Treshnikov, A. F. (1963), Features of the Antarctic Ocean regime, in *Tr. Sov. Antarkt. Eksped.*, vol. 21, Morskoi Transport Press, Leningrad.

Tressler, W. L., and A. M. Ommundsen, (1962), Seasonal oceanographic studies in McMurdo Sound, Antarctica, Tech. rep., U.S. Navy Hydrographic Office, Washington, D. C.

Trodahl, H., M. McGuinness, P. Langhorne, K. Collins, A. Pantoja, I. Smith, and T. Haskell (2000), Heat transport in McMurdo Sound first-year fast ice, *J. Geophys. Res.*, *105*(C5), 11,347–11,358, doi:10.1029/1999JC000003.

Wongpan, P., P. J. Langhorne, D. Dempsey, L. Hahn-Woernle, and Z. Sun (2015), Simulation of the crystal growth of platelet sea ice with diffusive heat and mass transfer, *Ann. Glaciol.*, *56*(69), 127–136, doi:10.3189/2015AoG69A777.

Wright, C. S., and R. E. Priestley (1922), *British (Terra Nova) Antarctic Expedition 1910–1913: Glaciology*, Harrison and Sons, London, U. K.

Zheng, S., J. Shi, Y. Jiao, and R. Ge (2011), Spatial distribution of Ice Shelf Water in front of the Amery Ice Shelf, Antarctica in summer, *Chin. J. Oceanol. Limnol.*, *29*(6), 1325–1338, doi: 10.1007/s00343-011-0318-x.